

Experimental and numerical study of corrugated anchors for CFRP plates

Jia-Qi Yang^{a,*}, Husheng Wang^a, Peng Feng^b, Guozhen Ding^c, Lili Wu^a

^a School of Mechanics and Civil Engineering, China University of Mining and Technology (Beijing), China

^b Department of Civil Engineering, Tsinghua University, China

^c Department of Civil and Environmental Engineering, Imperial College London, UK

ARTICLE INFO

Keywords:

CFRP plate
Corrugated anchor
Anchor efficiency
Prestress tendon

ABSTRACT

Carbon fibre-reinforced polymer (CFRP) plates are promising materials for cables and prestress tendons in structural engineering for the excellent tensile performance, light in weight and anti-corrosion character. Anchoring has always been the main challenge of this high-performance material due to its anisotropy and brittleness. Corrugated anchors are high-efficiency clamping-type anchorage devices. Nevertheless, premature failure of the CFRP plates can still be observed with this type of anchors, and the anchor efficiency for the corrugated anchors needs further improvement. This paper proposes a novel configuration of corrugated anchors. Experimental tests are then carried out to investigate the influence of the pre-tensioning bolt load and adhesive layer. Consequently, numerical analysis is conducted to reveal the anchoring mechanism. The results indicate the traditional corrugated anchors lead to non-uniform stress distribution in the CFRP plate, and with the proposed configuration the anchor efficiency can be increased up to 100 %.

1. Introduction

Carbon fibre-reinforced polymer (CFRP) is an emerging high performance material with high strength, light-weight and anti-corrosion characters [1]. In structural engineering, CFRP presents a promising alternative of steel for tensile elements such as cables or prestress tendons due to its excellent longitudinal tensile performance as well as the physical and chemical properties [2–4]. Usually, the CFRP tensile elements are fabricated via pultrusion technique that all carbon fibres are parallel to the longitudinal direction of the product with a constant cross section shape [2]. The early-stage discussion and pioneer application of CFRP cables are reported by Meier [5,6]. In addition, CFRP can be used as prestress tendons in flexural structural members, particularly for flexural strengthening of reinforced concrete beams [7–10].

Despite the aforementioned advantages, anchoring poses a significant challenge in the application of CFRP tensile elements. Different from steel, pultruded CFRP products are orthotropic which are strong in longitudinal but weak in transverse and shear [11]. Additionally, CFRP tends to fail in a brittle manner without allowing for stress redistribution [12]. When the tensile stress distribution within the CFRP section is non-uniform, shear stress will be generated, leading to premature failure instead of all fibres reach their ultimate strength simultaneously [10]. Therefore, the average stress of the anchored CFRP product at the

ultimate state is always lower than the material strength obtained from small sample test. Following Ai et al. [12], the anchor efficiency η is then defined as:

$$\eta = \sigma_u / f_{fcp} \quad (1)$$

where f_{fcp} is the CFRP strength from the material test, and σ_u is the ultimate strength of the anchored CFRP product which can be obtained from the test result by:

$$\sigma_u = F_u / A_n \quad (2)$$

F_u and A_n are the ultimate load and nominal section area of the anchored CFRP plate, respectively. Theoretically, the η has an upper limit of 1.0.

The fundamental anchoring mechanisms for CFRP materials include friction, chemical bond and mechanical interlock [13]. Essentially, anchoring is transmission of load between materials through their interface. Therefore, the specific surface area has strong influence on the anchor efficiency. The cross-section with higher specific surface area leads to larger effective load transmitting interface area. One method to increase the specific surface area is to use multiple small-diameter rods instead of single large-diameter rod, which is called “parallel-rod cable” [6,14,15]. Another effective approach involves the utilization of CFRP

* Corresponding author.

E-mail address: yangjiaqi@cumtb.edu.cn (J.-Q. Yang).

<https://doi.org/10.1016/j.conbuildmat.2024.138752>

Received 9 August 2024; Received in revised form 10 October 2024; Accepted 12 October 2024

Available online 19 October 2024

0950-0618/© 2024 Elsevier Ltd. All rights reserved, including those for text and data mining, AI training, and similar technologies.

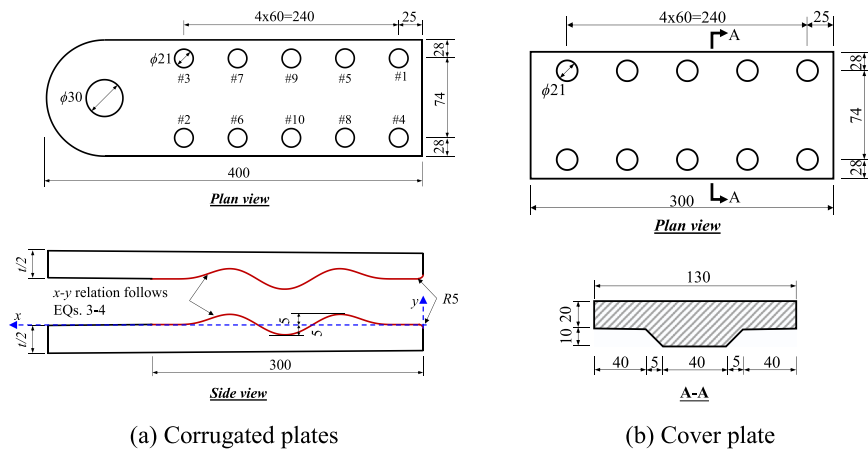


Fig. 1. Details of the anchors.

plates with rectangular cross-section that the width is significantly greater than the thickness. For instance, considering the typical commercially available CFRP plate product with 50 mm×1.4 mm rectangular section, its perimeter is approximately 3.5 times that of a CFRP rod with the same cross-section area. Due to the high specific surface area, CFRP plates have been widely used as prestress tendons in flexural strengthening [9,10]. In recent years, CFRP-parallel plate cables are developed [16,17] and firstly applied in the large-span roof of Sanya stadium in China [18].

The anchors developed for the CFRP plates include bond-type anchors [19], wedge-type anchors [20], clamping-type anchors [21–24] and self-anchored anchors [12,25]. Among various anchor configurations, clamping-type anchors are simple in structure and easy to install. Usually, clamping-type anchors compose of one or two steel plates, which is denoted as single-side clamping and double-side clamping herein. Single-side clamping anchors are usually used as the fixed anchor in flexural strengthening (e.g., Hosseini et al. [21] and Suter et al. [22]) that the clamping plate is bolted on the strengthened beam. For double-side clamping anchors, two steel plates are connected by bolts or rivets to clamp the CFRP plate, which is flexible to connect to prestressing devices (e.g., Andra et al. [23] and Piatek et al. [24]). The configuration of the clamping-type anchors enables the application of adhesion, and the pressure on the CFRP plate can be controlled by pre-tensioning torque of the bolts. Therefore, both bond and friction actions can be employed to enhance the anchor strength. In recent years,

corrugated anchors receive attention due to their capability to anchor not only single-layer but also multiple-layer plates [16,17,26]. Therefore, they can be used in both structural strengthening and CFRP parallel-plate cables [10,17]. The corrugated anchor was initially proposed by Zhuo and Li [27] and can be categorized as a clamping-type anchor, with friction being the primary anchoring mechanism. Analytical solutions suggest that the anchoring force is not only determined by the clamping force and friction coefficient, the shape of the corrugated anchor plates also have strong influence on the anchoring effect [27,28]. Consequently, if properly designed, its anchoring efficiency is higher than that of flat plate clamping-type anchors and wedge-type anchors.

However, there remain unresolved issues pertaining to the corrugated anchors. The previous study by the authors [10] found that the CFRP plate anchored by corrugated anchors exhibited premature failure with longitudinal cracks, indicating that there is non-uniform stress distribution within the CFRP plate. Existing analytical solutions are not able to explain this phenomenon because they simplify the anchor into a 2D model without considering the width of the plate [27,28]. In addition, there is lack of study on the effect of the clamping force and the application of adhesive layer. In this study, a novel configuration of the corrugated anchor is proposed. The influence of the pre-tensioning torque, plate thickness and adhesive layers are investigated experimentally. Finite element analysis is then conducted to reveal the mechanism of stress distribution in the CFRP plate. This study demonstrates that the proposed anchor effectively minimizes non-uniform stress distribution in CFRP plates and is able to achieve up to 100 % anchor efficiency.

Table 1

Details of test specimens.

Specimen ID	Plate thickness (mm)	Torque (N•m)	Adhesive	Impact analysis*			
				(a)	(b)	(c)	(d)
A20-T150-1-2	20	150	No	✓	✓	✓	✓
A20-T250-1-2	20	250	No	✓	✓	✓	✓
A20-T350-1-2	20	350	No	✓	✓	✓	✓
A20-T150b-1-2	20	150	Yes	✓	✓	✓	✓
A20-T350b-1-2	20	350	Yes	✓	✓	✓	✓
A30-T150-1-2	30	150	No	✓	✓	✓	✓
A30-T250-1-2	30	250	No	✓	✓	✓	✓
A30-T350-1-2	30	350	No	✓	✓	✓	✓
A30-T150b-1-2	30	150	Yes	✓	✓	✓	✓
A30-T250b-1-2	30	250	Yes	✓	✓	✓	✓
A30-T350b-1-2	30	350	Yes	✓	✓	✓	✓
B20-T150-1-2	20	150	No	✓	✓	✓	✓
B20-T250-1-2	20	250	No	✓	✓	✓	✓
B20-T350-1-2	20	350	No	✓	✓	✓	✓
B20-T250b-1-2	20	250	Yes	✓	✓	✓	✓
B20-T350b-1-2	20	350	Yes	✓	✓	✓	✓

* Notes: (a) influence of pre-tensioning torque; (b) influence of adhesive layer; (c) influence of anchor plate thickness; (d) influence of anchor type.

2. Experimental details

2.1. Design of test specimens

The primary aim of optimizing the anchoring device is to alleviate the non-uniform stress distribution across the CFRP plate section. Hence, this study investigates three parameters: anchor plate thickness, pre-tensioning torque, and application of epoxy adhesive. There are two types of anchors investigated in this study, namely, Type A and Type B. The Type A anchors consist of two steel plates with complementary corrugated surfaces which are cut from a single steel plate with thickness of t , so that each plate has a thickness of $t/2$. The shape of the corrugated surfaces is adopted from Ding et al. [29] with the coordinates shown by Fig. 1a:

$$y = \begin{cases} f(x - 25) & 25 \leq x \leq 150 \\ f(275 - x) & 150 < x \leq 275 \\ 0 & \text{otherwise} \end{cases} \quad (3)$$

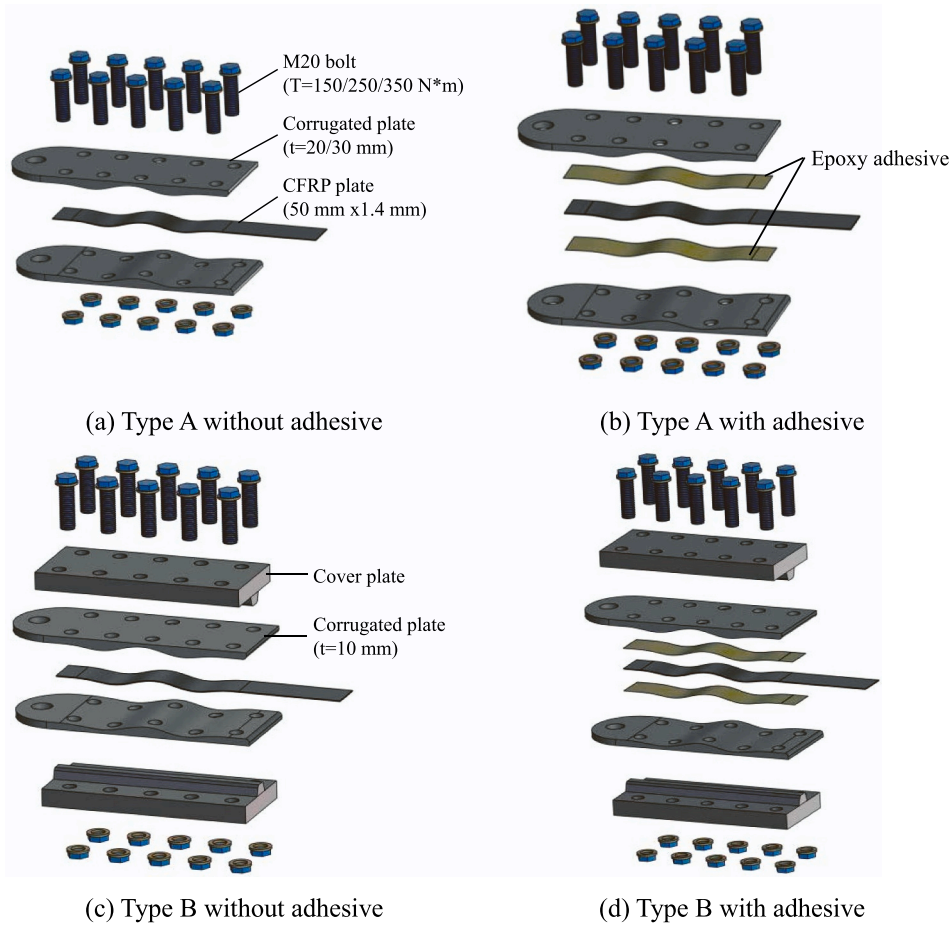


Fig. 2. Assembly of the anchors.

$$f(x) = 50 \left[\left(\frac{2x - 188}{188} \right)^2 - 1 \right]^3 \cdot \left(\frac{x - 94}{188} \right) \cdot \cos \left(\frac{\pi(x - 94)}{188} \right) \quad (4)$$

The two plates are fastened by ten $\phi 20$ bolts. In this study, plate thickness of $t=20$ mm and 30 mm are tested to investigate their influence on the anchoring performance. The dimensions of Type A anchors

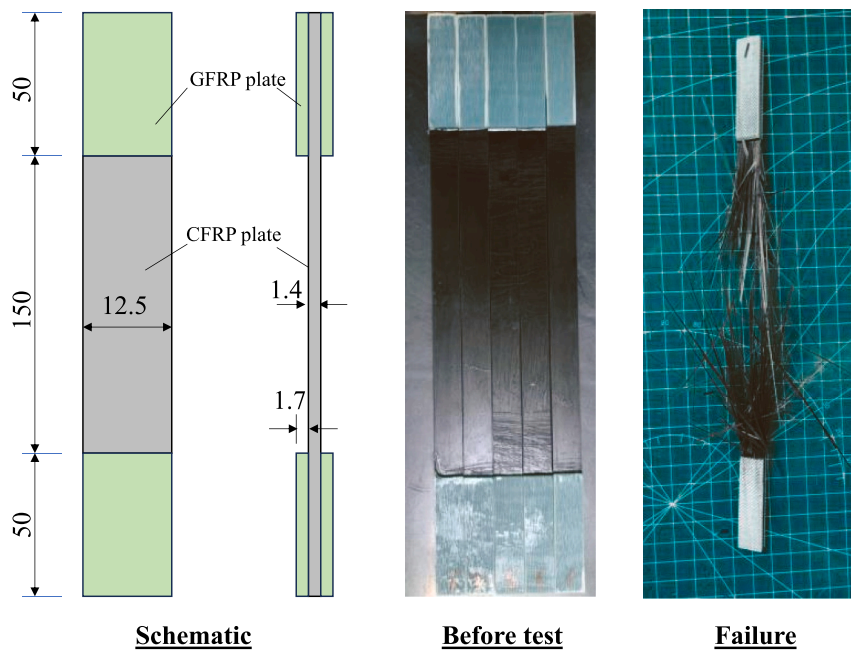


Fig. 3. Details of CFRP samples.

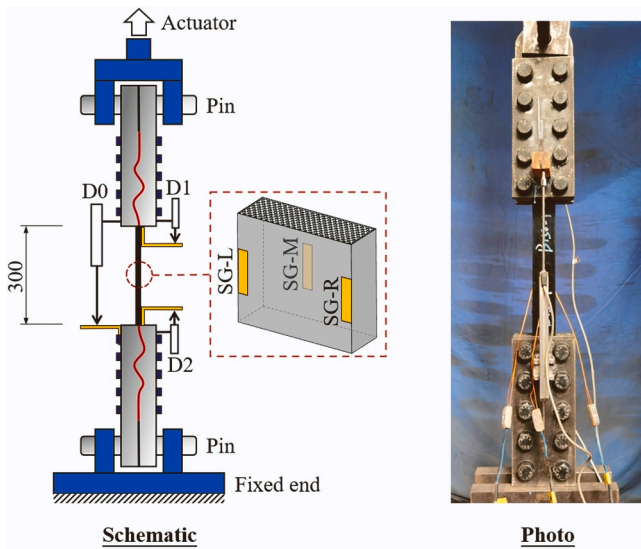


Fig. 4. Test setup.

are shown in Fig. 1a. For Type B anchors, the clamping pressure is applied to the $t=20$ mm corrugated plates via two cover plates positioned on both sides. The section of the cover plate is shown in Fig. 1b aiming at achieving a more uniform pressure distribution on the CFRP plate. Preliminary trial test results indicate that when the pre-tensioning torque $T \leq 100$ N·m, the anchor fails to provide adequate friction for the CFRP plate, resulting in the plate being pulled out from the anchor plates without damage. Therefore, the test plan includes $T=150, 250$ and 350 N·m as selected values. Besides, a two-part epoxy adhesive is applied to a portion of the specimens between the CFRP plate and the corrugated plates to investigate the anchoring performance with bond effect. In total, 16 sets of specimens have been prepared for the

experiment, with each set comprising two identical specimens. The details of the specimens are listed in Table 1. The specimens are labelled as [anchor type][plate thickness]-T[pre-tensioning torque][bond]-[number of specimen]. For instance, A30-T150-1 refers to Type A anchor with $t=30$ mm corrugated plates and 150 N·m pre-tensioning torque but without adhesive, while B10-T250b-1 is Type A anchor with 250 N·m pre-tensioning torque and adhesive. The assemblage of all test groups are shown in Fig. 2. For each specimen, the total length of the CFRP plate is 900 mm. The anchors are installed on both ends of the plate symmetrically with anchored lengths of 300 mm.

The preparation process of the test specimens are as follows: (1) Clean the contact surfaces of CFRP plate and steel anchor plates with alcohol; (2) Place the anchor plates and CFRP plate in a work fixture in sequence; (3) Insert and tighten the bolts manually with spanner until the CFRP plate is deformed and clamped by the anchor plates; (4) Tighten the bolts to 50 % of the target torque by torque wrench; and (5) Tighten all bolts to 100 % of the target torque. In steps (3)-(5), the bolts are tightened following the same sequence as shown in Fig. 1a. For bonded anchors, the epoxy adhesive is applied on both sides of the CFRP plate before step (2), and the specimen is cured at room temperature for at least 72 hours before test.

2.2. Material properties

The CFRP plates tested in this study have a nominal thickness of 1.4 mm and width of 50 mm which are manufactured by pultruding technique. Five coupon tests are carried out on the same batch of material in accordance with the Chinese standard GB/T3554-2014[30]. As shown in Fig. 3, the CFRP plate are cut into coupons with widths of 12.5 mm and lengths of 250 mm. Glass fibre-reinforced polymer (GFRP) plates of 1.7 mm thick were bonded on both ends of the coupon for local strengthening. All five specimens fail by fibre rupture as depicted in Fig. 3. The tested average elastic modulus $E_{fcp} = 147$ GPa (standard deviation, s.d.=1.8 GPa), and the ultimate tensile strength $f_{fcp} =$

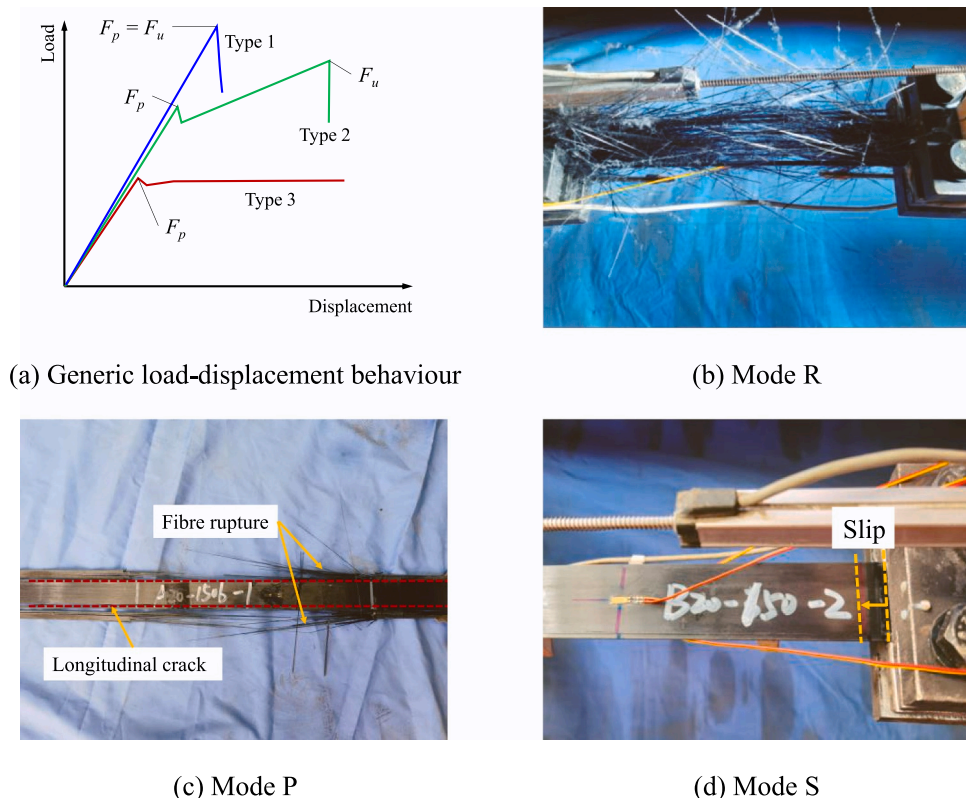


Fig. 6. Load-displacement relations and typical failure modes.

Table 2
Test results.

Specimen	σ_p	ave.	σ_u	ave.	η	Curve Type	Failure mode
A20-T150-1	1014	974	1014	974	44 %	Type 1	S
A20-T150-2	934		934			Type 1	S
A20-T250-1	1081	1131	1139	1160	52 %	Type 2	P+S
A20-T250-2	1180		1180			Type 1	P+S
A20-T350-1	1194	1139	1194	1199	54 %	Type 1	P
A20-T350-2	1083		1203			Type 2	P
A20-T150b-1	973	951	1247	1358	61 %	Type 2	P
A20-T150b-2	929		1469			Type 2	P
A20-T350b-1	1100	966	1570	1511	68 %	Type 2	P
A20-T350b-2	832		1452			Type 2	P
A30-T150-1	1093	1160	1287	1257	56 %	Type 2	P
A30-T150-2	1226		1226			Type 1	P
A30-T250-1	1096	908	1199	1208	54 %	Type 2	P
A30-T250-2	720		1217			Type 2	P
A30-T350-1	869	1083	1189	1268	57 %	Type 2	P
A30-T350-2	1296		1346			Type 2	P
A30-T150b-1	2044	2071	2044	2071	93 %	Type 1	P
A30-T150b-2	2098		2098			Type 1	P
A30-T250b-1	1051	997	1362	1359	61 %	Type 2	P
A30-T250b-2	943		1356			Type 2	P
A30-T350b-1	1139	1096	1448	1508	68 %	Type 2	P
A30-T350b-2	1053		1567			Type 2	P
B20-T150-1	884	917	884	917	41 %	Type 3	S
B20-T150-2	950		950			Type 3	S
B20-T250-1	1936	1852	1936	1852	83 %	Type 2	P+S
B20-T250-2	1768		1768			Type 2	P+S
B20-T350-1	2042	1805	2042	2028	91 %	Type 1	P
B20-T350-2	1568		2013			Type 2	P
B20-T250-1b	2040	2044	2258	2153	97 %	Type 2	P
B20-T250-2b	2047		2047			Type 1	P
B20-T350-1b	2708	2572	2708	2572	115 %	Type 1	R
B20-T350-2b	2435		2435			Type 1	R

2227 MPa (s.d.=123 MPa). The M20 bolts are of grade 10.9, and all the anchor plates are made of Q355 steel with characteristic yield strength of 355 MPa. The properties of the bolts and steel plates are not tested because they are less concerned in this study.

2.3. Test setup

The specimens are tested in tension. The specimen is connected to the test rig via two $\phi 28$ pins on both ends as shown in Fig. 4. Three linear variable differential transformers (LVDTs), namely D0, D1 and D2, are installed to measure the deformation. D0 measures the total deformation between the anchors on both ends, while D1 and D2 measure the local slip of the CFRP plate at the entrance of the anchors. The range of D0 is 100 mm with accuracy of 0.1 mm. The ranges of D1 and D2 are 25 mm with accuracy of 0.0625 mm. Three strain gauges, namely SG-L, SG-R and SG-M are installed in the middle of the CFRP plate. SG-L and SG-R lay on both edges of the plate, and SG-M is installed along the centre line on the opposite side. The strain gauges are 120 Ω -10AA with ranges of 20000 $\mu\epsilon$ and accuracy of 5 $\mu\epsilon$. The load is force controlled by 5 kN/min before the peak load. After the peak load, which is often accompanied by load drop and damage of the specimen, the load is changed to manually controlled until total loss of strength.

3. Experimental results

3.1. General behaviour and failure modes

The load-displacement curve (measured by D0) for the test specimens can be categorized to three typical types as schematically illustrated in Fig. 6a. Initially, the load-displacement curves are linear with the slope close to that of the CFRP plate stiffness, indicating the elastic behaviour of the anchoring system. Type 1 curve presents a typical brittle failure mode that there is a total loss of strength after reaching the peak load (F_p). Consequently, the peak load is the same with the ultimate load (F_u). For Type 2 curves, the CFRP plate exhibits initial damage at the first peak load (F_p) with or without drop of load. After the plate damage, the load can increase with a reduced stiffness until the ultimate load (F_u) prior to failure. For Type 3 curves, after the first peak load, the load does not change with the increase of the displacement, which always exhibits slip between the CFRP and the anchor plates. The ultimate strength (σ_u) is defined in Eq.2, and the peak strength (σ_p) can be calculated as follows:

$$\sigma_p = F_p/A_n \quad (5)$$

where A_n is the nominal CFRP plate section area which is 70 mm². The results of σ_p , σ_u and the type of the load-displacement behaviour are listed in Table 2. There are three basic failure modes observed in the test, namely: (1) complete fibre rupture (noted as Mode R shown in Figs. 6b), (2) partial failure (noted as Mode P shown in Fig. 6c), and slip (noted as Mode S shown in Fig. 6d). The failure mode for an individual test specimen may manifest as one or a combination of the three basic modes. In this study, Mode P is most frequently observed. In this mode, the longitudinal cracks emerge on the CFRP plate near both edges when the load reaches F_p . Meanwhile, the fibre on both edges of the CFRP plate start to rupture. This phenomenon is always accompanied by a partial loss of strength. If the unruptured part of the CFRP plate can withstand a higher load, the specimen will exhibit Type 2 behaviour. Otherwise, it will demonstrate Type 1 behaviour. There are two scenarios in which Mode S are observed: First, there is inadequate friction force acting on the CFRP plate, leading to Type 3 curve with a friction-slip plateau. Second, in the event of partial failure, the strain energy suddenly releases and the remaining part of the CFRP plate is subjected to impact action, which results in the slippage of the CFRP plate. In the latter scenario, Type 1 or Type 2 behaviour can be observed. Mode R is the most brittle failure mode, characterized by simultaneous fibre rupture of the entire CFRP plate section. Specimens fail in this mode exhibit Type 1 behaviour. This is the most desirable failure mode because the material in the whole section reaches its ultimate strength simultaneously and the anchor efficiency is maximized. The failure modes for all specimens are listed in Table 2.

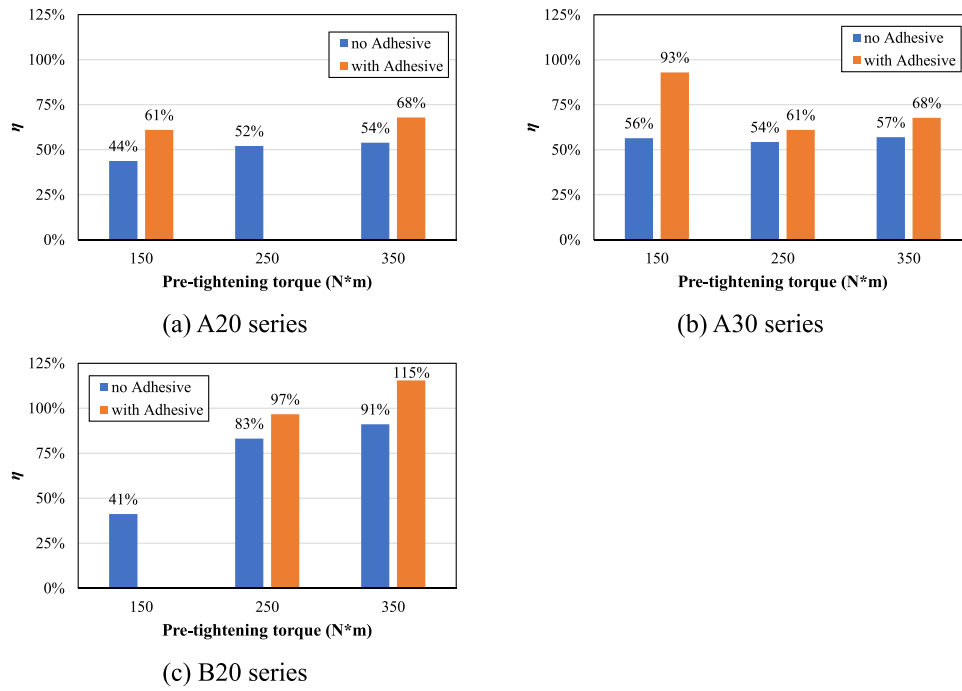


Fig. 7. Anchor efficiency.

3.2. Anchor efficiency

The average anchor efficiencies for each group are listed in Table 2, and are plotted in Fig. 7 as well. For all unbonded Type A anchors, the values of η range from 44 % to 57 %. As can be observed in Figs. 7a and 7b, neither increasing the pre-tensioning torque nor the anchor plate thickness has significant effect in enhancing the anchor efficiency for Type A anchors. When using Type B anchors, however, η reached up to

91 %, with the influence of pre-tensioning torque being more pronounced as shown in Fig. 7c. The presence of the epoxy adhesive enhances the anchor efficiency in all tested groups. Particularly, the B20–350b series achieve an average of anchor efficiency of 115 %, which is highest among all test specimens. The increase in η resulting from the adhesive shows weak correlation with the pre-tensioning torque. As shown in Fig. 7, for the A20 and B20 series, the epoxy adhesive has better performance when the torque is higher. However, for the A30

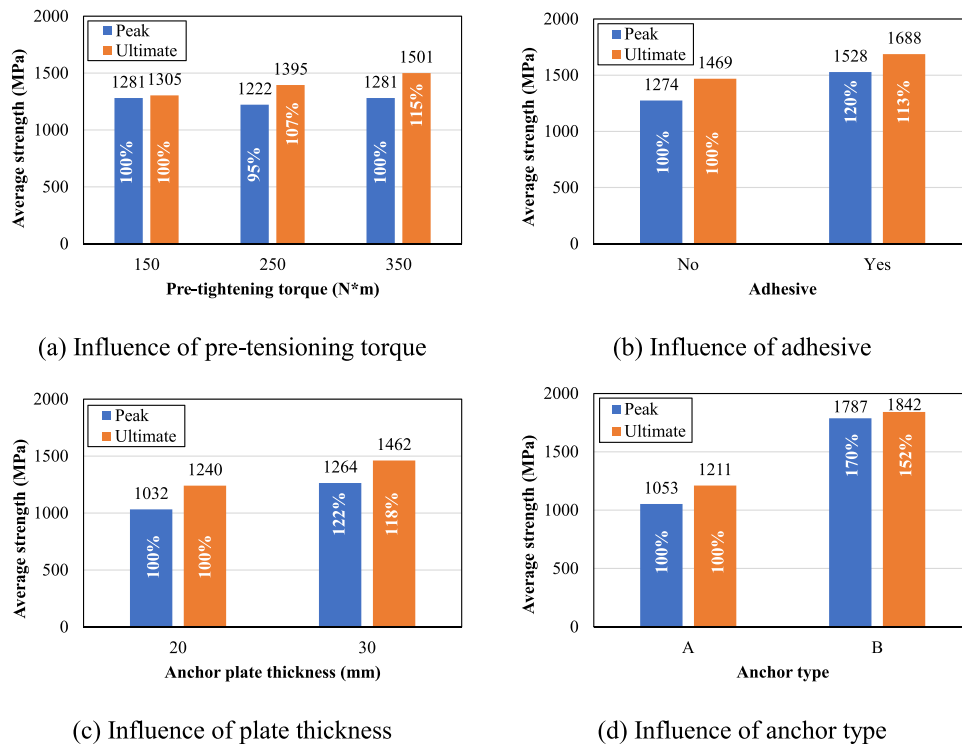


Fig. 8. Influence of the test parameters.

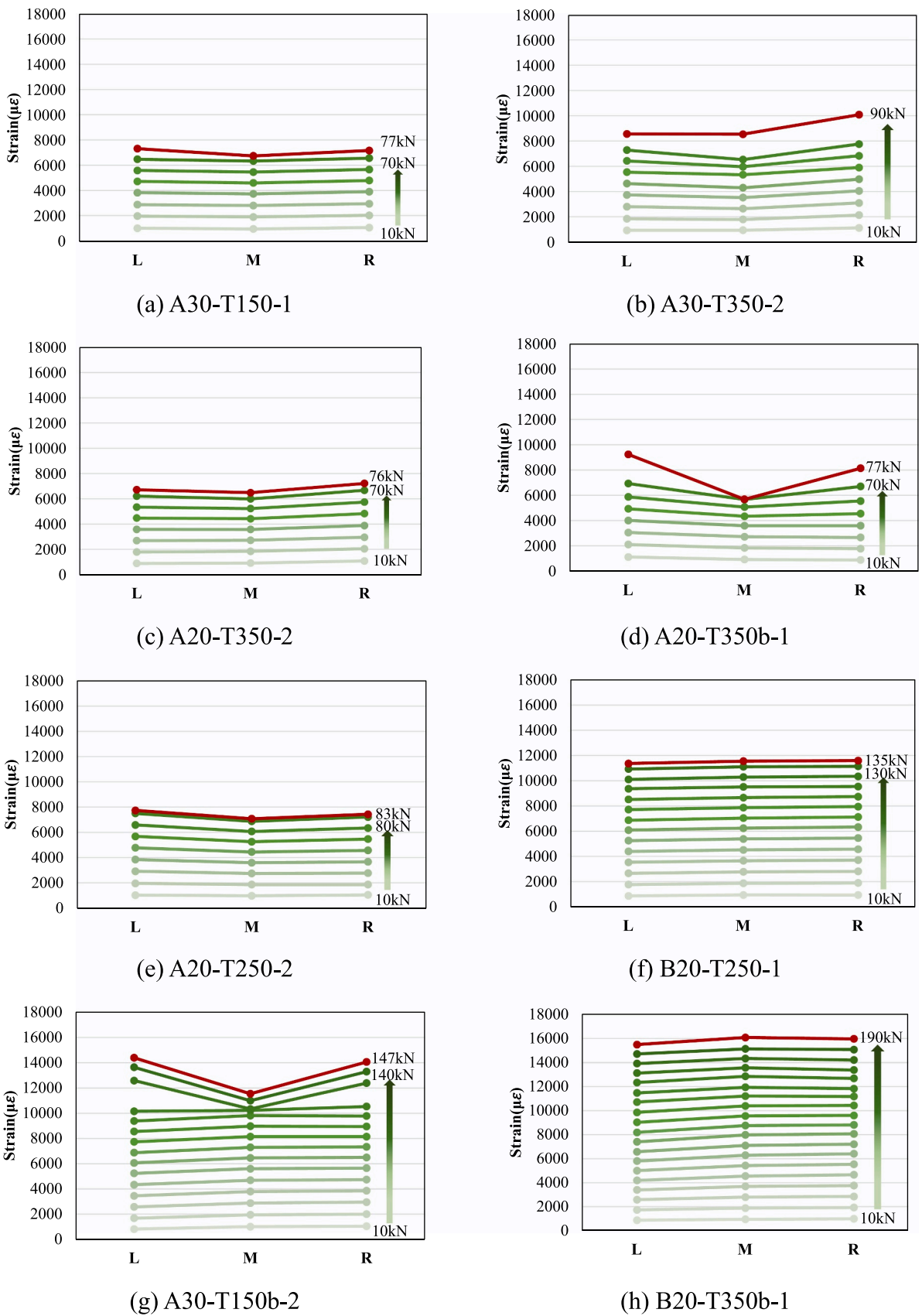


Fig. 9. Selected strain results.

series, the adhesive layer performs best when $T = 150 \text{ N}\cdot\text{m}$, which achieves 93 % of the anchor efficiency. For summary, application of both cover plates and adhesive are effective solutions for maximizing the anchor efficiency, and B20–350b is the optimum anchor configuration which has $\eta=115 \%$. This configuration enables the full utilization of the material strength of the CFRP plate. It is worth noting that η is calculated with the tested $f_{fp}=2227 \text{ MPa}$, which is lower than the manufacturer provided CFRP strength (2400 MPa). This indicates that the quality of this batch of CFRP plate is not stable. Nevertheless, no matter which value is adopted in Eq. 1, the η values for B20–350 series exceed 100 %, which verifies the success of the novel anchor configuration, and the test results can also support all other conclusions made by this paper.

3.3. Impact analysis of the test parameters

To examine the impact of individual test parameters on the peak strength (σ_p) and the ultimate strength (σ_u), the concept of average strength is introduced herein. When analysing the influence of a specific factor, all test results are divided into two or three groups with respect to the concerned parameter, and average values of σ_p and σ_u are taken from the results of each group, which are noted as $\sigma_{p,ave}$ and $\sigma_{u,ave}$, respectively. As the test is not designed as a perfect orthogonal experiment, certain test data are excluded when analysing a single parameter in order to maintain the constant weight of all other factors. Details of the grouping are listed in Table 1. The results are plotted in Fig. 8. It should be noted that the trend of the average strengths with respect to the concerned parameter holds greater significance than the values themselves. Therefore, in each graph of Fig. 8, the results of both $\sigma_{p,ave}$ and $\sigma_{u,ave}$ in first group are marked as 100 %, and the results from the rest group(s) are normalized by dividing their counterpart in the first group, which are also marked on the bars in the column chart. According to Fig. 8a, the pre-tensioning torque has no significant influence on the $\sigma_{p,ave}$, and has positive but limited influence on the $\sigma_{u,ave}$. This is consistent with the previously presented results. The presence of the adhesive layer is more effective in increasing the $\sigma_{p,ave}$. It enhances the $\sigma_{p,ave}$ and $\sigma_{u,ave}$ by 20 % and 13 % compared with the unbonded specimens as shown in Fig. 8b. The influence of the anchor plate thickness yields different conclusion with the anchor efficiency results. For the same Type A anchor plates, the thick plate group achieves the $\sigma_{p,ave}$ and $\sigma_{u,ave}$ with 22 % and 18 % higher than the thin plate group, respectively. The statistical findings indicate that increasing the anchor plate thickness is an effective approach to improve the anchor performance. This contradiction mainly attributes to the results of A30–150b series, which will be discussed later in this paper. Among all the test parameters, the use of the cover plate (type B anchor) is the most effective way in maximizing the anchorage strength. Compared with the Type A anchor group, the $\sigma_{p,ave}$ is increased by 70 %, and the $\sigma_{u,ave}$ is increased by 52 %, which is shown in Fig. 8d. The use of cover plate alters the pressure distribution on the CFRP plate, thereby addressing the issue of non-uniform stress distribution, which will be discussed later in this paper. Therefore, Type B represents the recommended anchor configuration for corrugated CFRP plate anchors.

3.4. Strain analysis

The tensile strain distributions obtained from the strain gauges of selected specimens are plotted in Fig. 9. The strains are illustrated at intervals of every 10 kN of the tensile load, denoted by green lines in the figure. When the load reached F_p , the corresponding strain results are plotted in the figure as well, which are highlighted with red lines. After reaching F_p , the specimens may undergo plate damage, such as longitudinal cracking or fibre rupturing. After this point, the strain gauge results become unreliable and are therefore not further analysed.

For Type A anchors, increase in the pre-tensioning torque leads to a higher total clamping force, which has positive influence on the anchorage strength. However, it exacerbates the non-uniformity of the

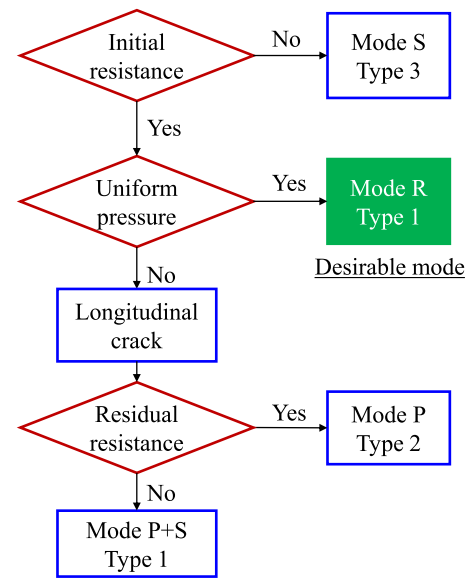


Fig. 10. Influencing factors for anchor behavior.

pressure on the CFRP plate, exerting a negative effect for the anchorage performance. This can be observed from Figs. 9a and 9b. Therefore, for Type A anchors, the pre-tensioning torque should not be too small that is not sufficient to resist the CFRP from slipping, and it also should not be too large to result in severe stress concentration as well. Therefore, there exists an optimum pre-tensioning torque for Type A anchors.

Increasing the thickness of the anchor plate was intended to alleviate the non-uniform strain distribution. As can be observed from Figs. 9b and 9c, however, the specimen with thicker anchor plate has limited improvement on the strain distribution. This conclusion is consistent with the discussion in Section 3.2.

As shown in Figs. 9c and 9d, the two specimens have almost the same strain distributions when $F = 70 \text{ kN}$. With the presence of the adhesive layer, the A20-T350b-1 specimen can withstand more pronounced strain non-uniformity at F_p . Also, its ultimate strength is 30 % higher than A20-T350-2. Therefore, the adhesive layer can provide extra resistant force to the CFRP plate especially after the initiation of damage. However, it is less effective in alleviating the strain concentration is limited.

The stress distribution in the CFRP plate is significantly altered by the presence of the cover plates, which can be seen from Figs. 9e and 9f. The strains on the edges of A20-T250-2 specimen start to deviate from that of the middle section at $F = 50 \text{ kN}$. However, for the B20-T250-1 specimen, the strains at the three points remain close to each other before the load reaches F_p . The strain distribution indicates that the Type B anchors can achieve a uniform deformation across the CFRP plate at a higher load level.

Figs. 9g and 9h present the best performances for Type A and B anchors, respectively. The strain distribution of the A30-T150b-2 specimen remains uniform when $F=110 \text{ kN}$ with strain of around $10000\mu\epsilon$. Afterwards, the strains on the edges grow more quickly than that in the middle until the occurrence of shear damage, and the specimen finally fail in Mode P. For the B20-T350b-1 specimen, the strains at the three points are closed to each other during the entire loading process and reached or exceeded the ultimate tensile strain of the material (i.e. $15149\mu\epsilon$). This specimen fails by Mode R.

For summary, the factors influencing the failure modes and load-displacement curve types are illustrated by the flow chart as shown by Fig. 10, and the mechanisms for the anchor behaviour are explained as follows: (1) Adequate resistant force must be present to prevent the pull-out of the CFRP plates, otherwise it will result in Mode S and Type 3 curve with low anchoring strength; (2) If the pressure applied on the CFRP plate is not uniform, the plate will damage in shear during the test,

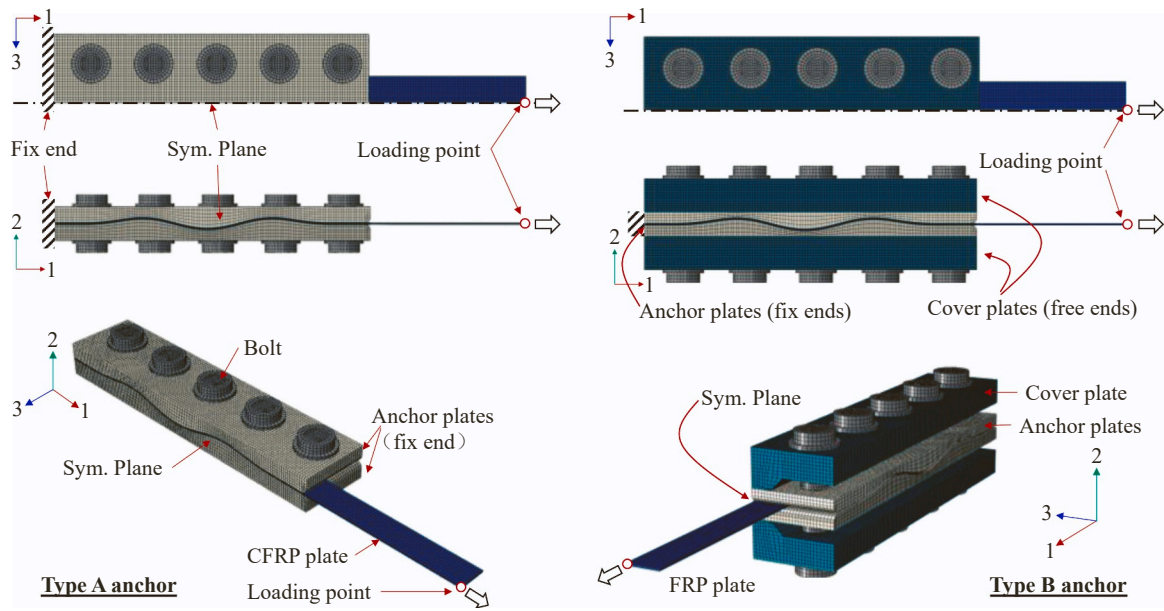


Fig. 11. Finite element model.

and the two edges of the plate starts to fracture, which is classified as Mode P. If the anchor can provide sufficient slipping resistance to the remaining CFRP plate, the load can increase to a higher value and the anchor will have a Type 2 behaviour, otherwise the remaining part of the CFRP plate will be pulled out under the impact load caused by the partial fracture; (3) With both sufficient slipping resistance and uniform pressure distribution, the specimen will fail in Mode R with Type 1 behaviour, which is the most desirable failure mode.

Therefore, when designing a corrugated CFRP plate anchor, two key issues need to be concerned: (a) provide sufficient resistant force against slipping, and (b) apply uniform pressure on the CFRP-steel interface. Due to the configuration of Type A anchors, though increasing the pre-tensioning torque can increase the resistant force against slipping, but it will lead to more severe stress non-uniformity. Therefore, the exceptional performance of the A30-T150b series can be explained as follows: the presence of the adhesive layers provides sufficient resisting force to the CFRP plate, meanwhile the thicker anchor plates and smaller pre-tensioning torque lead to less stress concentration. Hence this series performs best among all Type A anchors.

4. Finite element analysis

4.1. FE modelling

In this section, finite element analysis is conducted via ABAQUS to further investigate the mechanism of the corrugated anchor. Due to symmetry, 1/4 of the test specimens are modelled with 8-node 3D solid elements with reduced integration C3D8R. The FE model consists of CFRP plate, adhesive layers, anchor plates and bolts, which is shown in Fig. 11. Following Ding et al. [31], the characteristic element size is chosen to be 2.5 mm. All steel elements including steel plates and bolts are defined as linear elastic isotropic material with elastic modulus $E_s = 206$ GPa and Poisson's ratio $\nu_s = 0.3$. The elastic modulus of adhesive layer (E_a) for the bonded anchors is 3558 MPa, and the Poisson's ratio $\nu_a = 0.3$. The CFRP plates are set as transverse isotropic material. The longitudinal modulus $E_L = 147$ GPa which is obtained from the tensile test of the CFRP coupons. Since there is lack of test results of the rest of the material parameters, they are adopted from Liu et al. [11]. According to the pilot parametric study conducted by the authors, the transverse and shear properties do not have significant influence on the analysis results. Therefore, these parameters are used in this study to

Table 3
Material properties for CFRP plates.

E_L (GPa)	E_T (GPa)	G_{LT} (GPa)	G_T (GPa)	ν_{LT}	ν_T
147	12	9	6	0.3	0.33

model the CFRP plates, as listed in Table 3. In the FE model, the adhesive layer and the CFRP plate share nodes at the interface, implying perfect bond between these two materials. The thickness of the adhesive layer is 0.2 mm following Ding et al. [31]. The friction coefficient for steel-to-steel and steel-to-adhesive interfaces are set as 0.2 and 0.25 [32], respectively. The normal behaviours of these two interfaces are defined as hard contact. The end of the anchor plates is fixed, and all symmetry planes are assigned with corresponding symmetrical boundary conditions. The nodes at the section of the CFRP plates are coupled to a loading point locates at the intersection of z- and x- symmetry plane, which lies at the centre of the test specimen.

The analysis procedure is divided into four steps considering both convergency and computational cost. First, pre-tensioning load of 100 N is assigned to each bolt to ensure all parts of the model are in contact; Then the bolt load is increased to the target value according to the pre-tensioning torque levels, which is calculated in accordance with the handbook of mechanical design [33]; Subsequently, the loading point is moved 1 mm to the x direction to eliminate initial slip between interacting surfaces; Finally, the loading point is moved to the x direction

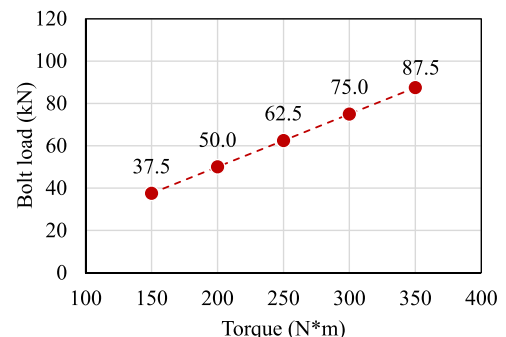


Fig. 12. Bolt load levels.

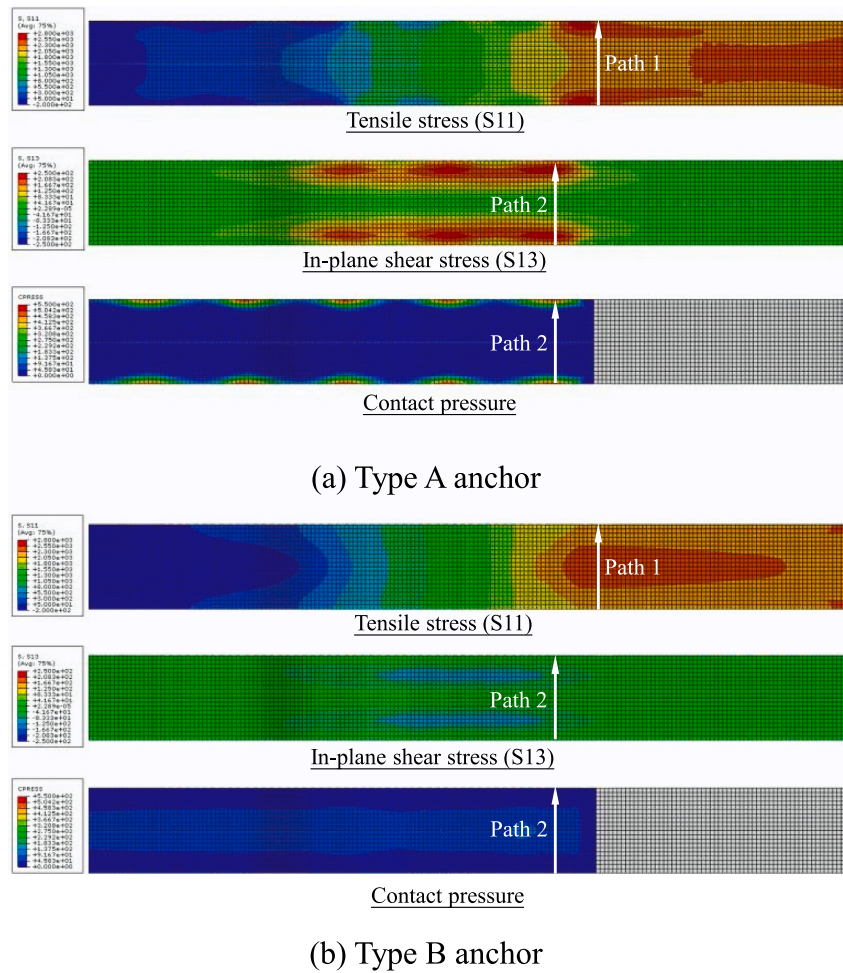


Fig. 13. Typical stress distributions on the CFRP plates.

until the reaction force of the loading point reaches 78 kN, which means the average tensile stress in the CFRP plate reaches the ultimate tensile strength $f_{frp}=2227$ MPa. It is worth noting that in this analysis, the CFRP plate is linear elastic without assigning damage criteria. Therefore, the stress in the plate may exceed the ultimate strength of the material. Nevertheless, it is still able to highlight the regions that prone to damage, and can back calculate the ultimate load.

In the FEA program of Type A anchors, the pre-tensioning torque (T) is varied from 150 N-m to 350 N-m with a 50 N-m increment for each level (5 levels in total, see Fig. 12), and the total thickness of the corrugated anchor plate (t) is varied as 20, 30, 40 and 50 mm (4 levels in total). Together with the bonded/unbonded scenarios, 40 models are built for analysis. For Type B anchors, the five levels of torque and

bonded/unbonded scenarios are consistent with Type A, and the plate thickness of 20 and 30 mm are investigated. Hence, there are 20 models in total for Type B anchors.

4.2. Results and discussions

The stress contours on the FRP plate are presented in Fig. 13, including longitudinal tensile stress (S11), in-plane shear stress (S13) and contact pressure (S22). Fig. 13 shows the two basic modes of stress contours, which are obtained from model A20-T250 and B20-T250, respectively. For each model, two key paths are defined across the CFRP plate sections, which are also plotted in Fig. 13. Path 1 locates at the entrance of the anchor plate along which the S11 is extracted. Path 2

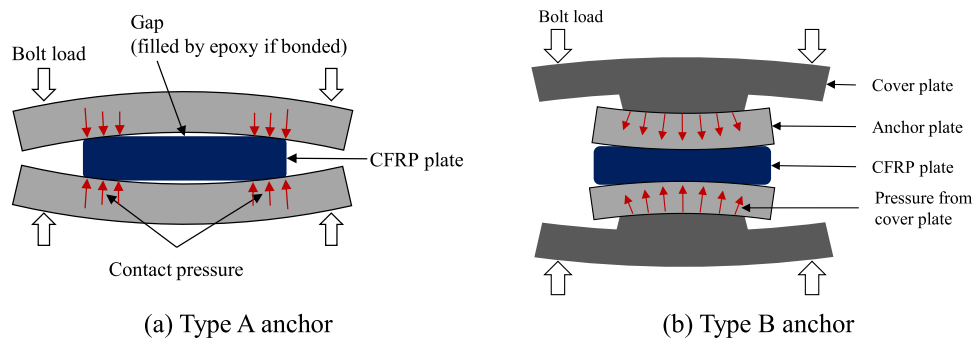


Fig. 14. Mechanism of contact pressure distribution.

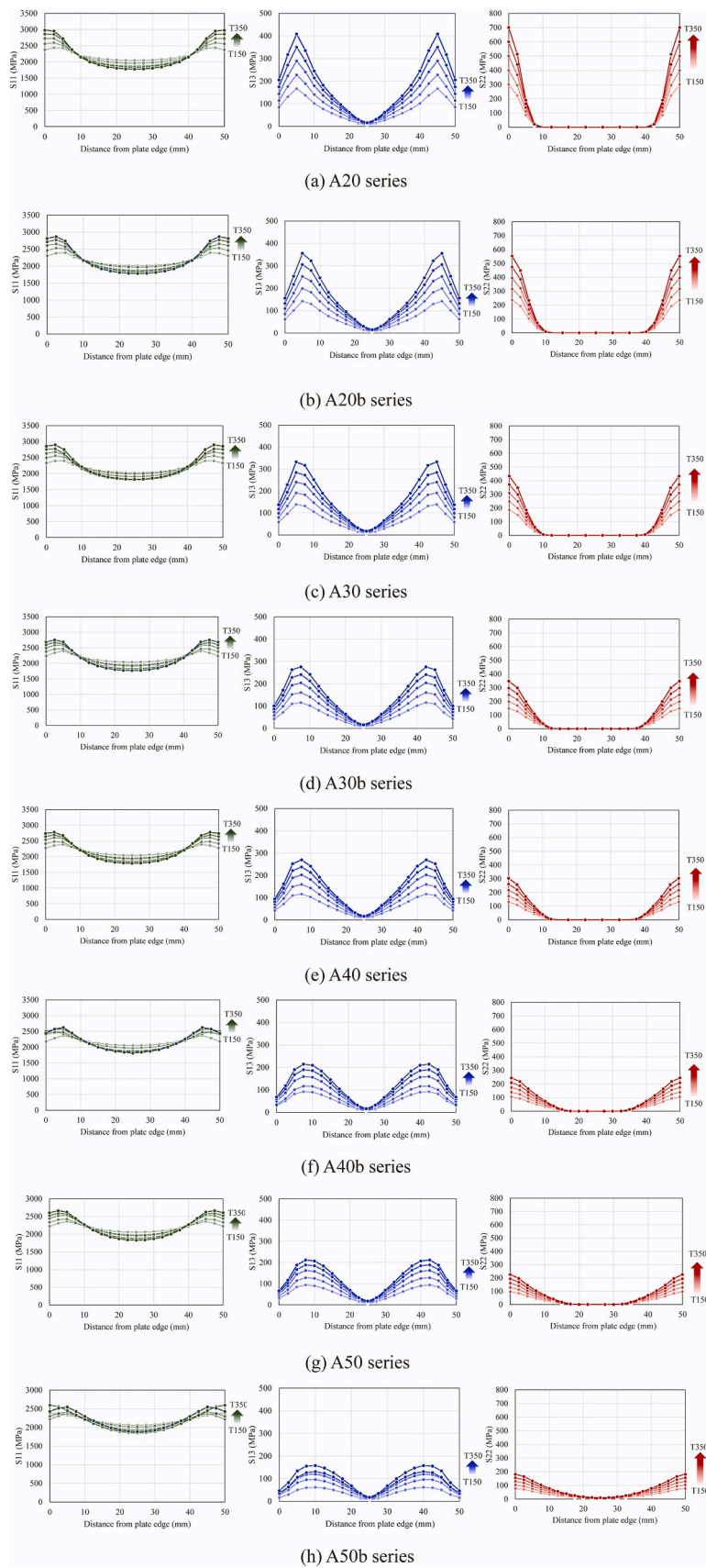


Fig. 15. Stress distributions for Type A anchors.

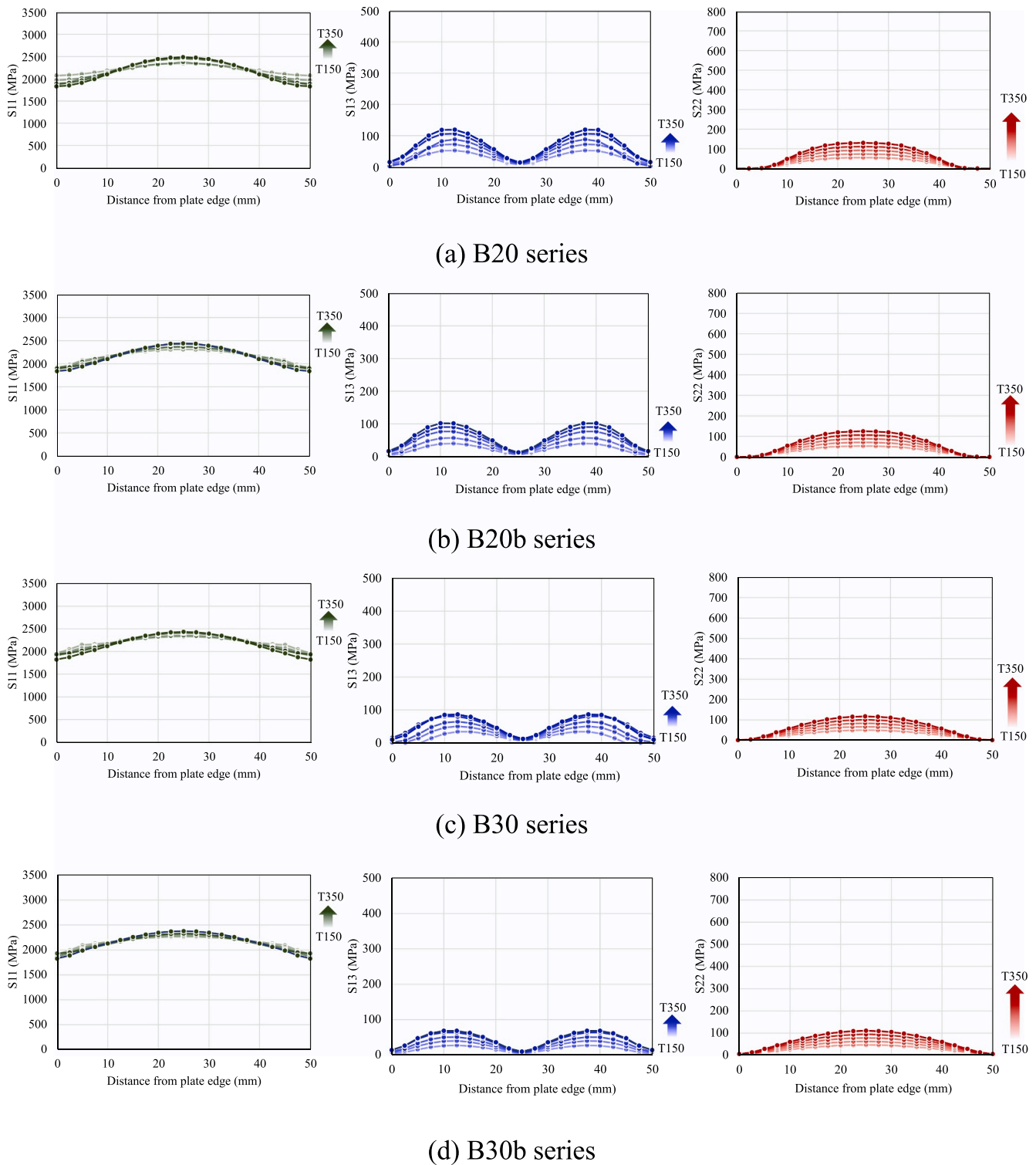


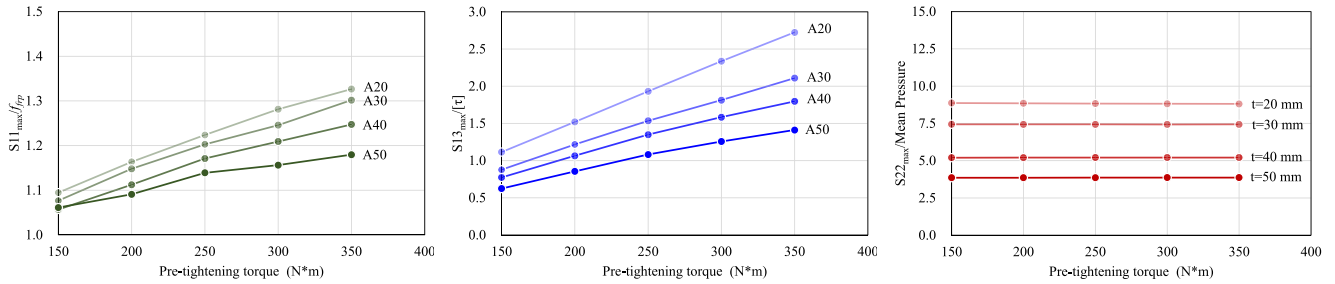
Fig. 16. Stress distributions for Type B anchors.

locates along the first row of bolts, where maximum values of S13 and S22 can be captured.

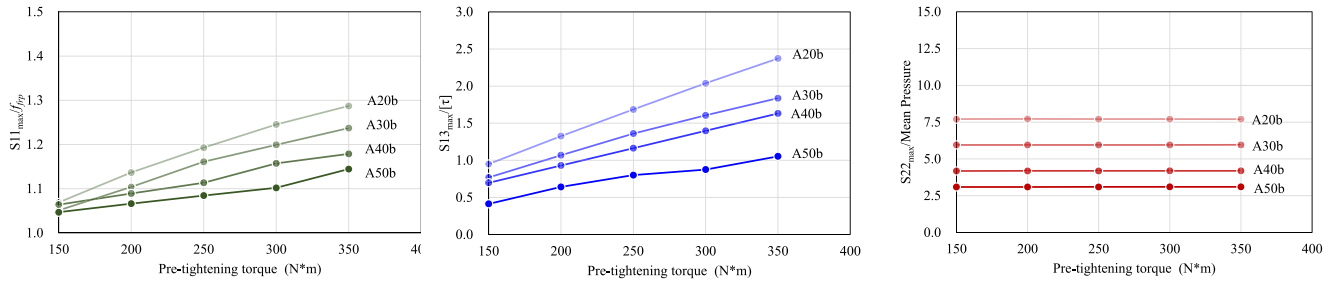
4.2.1. Influence of anchor type

For Type A anchor (Fig. 13a), the tensile stress (S11) concentrates at both edges of the CFRP plate, and there are two shear bands near the edges. This is attributed to the anchor configuration. When the bolts are tightened, the corrugated anchor plates exhibit out-of-plane bending deformation which is demonstrated schematically by Fig. 14a, resulting

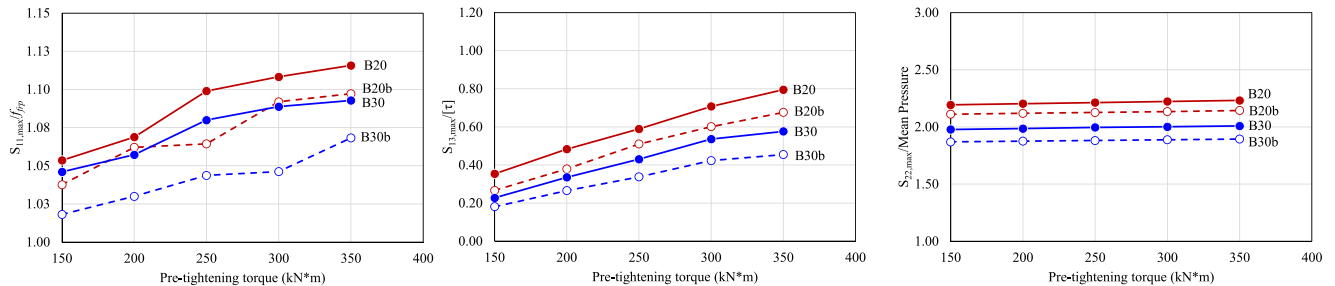
in pressure (S22) concentration at the positions of the bolts. It can also be seen from Fig. 15 that the maximum S11 locates at 0 or 2.5 mm to the edges, and the peak S13 occurs at about 5 mm from the plate edge. Also, the S22 is very high at both edges, but is zero in the middle of the plate section. The non-uniform pressure distribution results in higher friction and tensile stress at the edges but lower in the centre, hence generates the in-plane shear stress. Once the shear stress exceeds the shear strength of the CFRP plate $[\tau]$, longitudinal cracks form inside the anchored area and propagate along the CFRP plate. Meanwhile, the



(a) Maximum stresses for Type A anchors without adhesive



(b) Maximum stresses for Type A anchors with adhesive



(c) Maximum stresses for Type B anchors

Fig. 17. Influencing factors on maximum stresses.

concentrated tensile stress causes premature fibre rupture at both edges. This is the mechanism for the Mode P failure of Type A anchors, which is consistent with the test observations.

For the Type B anchors shown in Fig. 13b, the stress concentration is significantly relieved due to the presence of the cover plate. Different from the Type A anchors, the S11 is higher at the middle of the section than that at the edges. Though there are two shear bands occur on the CFRP plate, the absolute value is much smaller comparing to that in Fig. 13a. The stress results along key paths are plotted in Fig. 16. The maximum S11 occurs in the middle of the section and changes smoothly along the path. Therefore, the peak value of S13 is lower than that of the Type A anchors. Similar with the S11, the maximum S22 locates at the centre of the section and gradually decreases to zero at the edges. The effective clamping zones are at least 30 mm in the middle of the CFRP plate, which is just opposite to the Type A anchors. This result confirms the efficiency of the use of the cover plate. With the bulged cover plate, the clamping pressure is applied on the corrugated anchor plates indirectly via contact. Therefore, the anchor plates exhibit less bending action and can spread the pressure onto the CFRP plate surface more uniformly, as is shown by Fig. 14b.

4.2.2. Influence of pre-tensioning torque

In Figs. 15–16, the stresses along key paths of CFRP plate sections are

demonstrated by series of curves with respect to different levels of pre-tensioning torques. For each case, the peak values of all three concerned stresses increase with the torque. For Type A anchors, the higher torque causes larger out-of-plane bending deformation of the anchor plate, and therefore enhances the pressure concentration on the edges and results in higher shear stress. For Type B anchors, the influence of the torque is less significant due to the anchor configuration. The effects of the pre-tensioning torque are also demonstrated by Fig. 17. In the figures, the maximum tensile stress on Path 1 ($S_{11,max}$) is normalised by dividing the tensile strength of the CFRP plate (f_{fp}), which is 2227 MPa from the material test. The maximum in-plane shear stress on Path 2 ($S_{13,max}$) is normalised by dividing the shear strength $[\tau]=150$ MPa. Due to lack of test data, $[\tau]$ is obtained from Liu et al. [11]. The maximum pressure on Path 2 is normalised by dividing the nominal mean pressure, which is the total bolt load divided by the projected contact area ($300 \text{ mm} \times 50 \text{ mm} = 15000 \text{ mm}^2$). According to Fig. 17, the normalised $S_{11,max}$ and $S_{13,max}$ increase with the torque, and the influence on the normalised $S_{22,max}$ is minor. This indicates that the torque only affects the scale of the pressure, but cannot change its distribution mode.

4.2.3. Influence of plate thickness

As shown in Fig. 14a, the stress concentration of Type A anchor is caused by the bending of the anchor plate. Therefore, when the anchor

plate is thinner, the contact pressure concentrates at the edges, and there is wider pressure-free zone in the middle of the CFRP plate section. By increasing the plate thickness from 20 mm to 50 mm, $S11_{max}$ is reduced by up to 12 %, $S13_{max}$ is reduced by up to 67 %, and $S22_{max}$ is reduced by up to 60 % (see Fig. 17a). Therefore, increasing the plate thickness is effective in reducing the peak shear stress and contact pressure, but less effective in alleviating the tensile stress concentration.

For the Type B anchors, the influence of the plate thickness is similar with the Type A anchors. By increasing the plate thickness from 20 mm to 30 mm, $S11_{max}$ is reduced by up to 3 %, $S13_{max}$ is reduced by up to 36 %, and $S22_{max}$ is reduced by up to 12 %. For the same plate thickness levels in Type A anchors, the values are 4 %, 23 % and 23 %, respectively. Though increasing the anchor plate thickness can effectively reduce the shear stress, there is no need to further increase it because the shear stresses in the CFRP plate are far less than $[\tau]$ and no shear failure would occur.

4.2.4. Influence of adhesive

For Type A anchors, by adding the adhesive layer, the average reduction rates for $S11_{max}$, $S13_{max}$ and $S22_{max}$ are 3 %, 16 % and 16 %, respectively, and the values for Type B anchors are 2 %, 19 % and 6 %, respectively. The presence of the adhesive layer can reduce the shear stress for both types of anchors. It is also effective in alleviating the pressure concentration in Type A anchors.

In summary, using the cover plate is the optimum solution for enhancing the anchor efficiency. Increasing the plate thickness and introducing adhesive layer also have positive effect in relieving the stress concentration. Increasing the pre-tensioning torque, however, is negative to the anchor performance especially for the Type A anchors because it introduces higher shear stress which can cause premature shear failure before fibre rupture. The FE analysis yields equivalent conclusions with the test.

5. Conclusions

In this work, experimental tests were conducted on the anchorage performance of corrugated anchors for CFRP plates. The influences of pre-tensioning torque, anchor plate thickness as well as adhesive layer were investigated experimentally. Additionally, a novel type of corrugated anchor with bulged cover plate was proposed and tested, which improved the anchor efficiency up to 100 %. Furthermore, finite element analysis was performed to further unveil the anchoring mechanism and stress distribution. The following conclusions can be drawn from this study:

- (1) The configuration of the conventional corrugated anchors (Type A anchors) inevitably leads to non-uniform pressure distribution on the CFRP plate. Although increasing the anchor plate thickness and incorporating adhesives can mitigate stress concentration, it will bring extra problems in fabrication, transportation and construction.
- (2) For Type A anchors, once the clamping force is sufficient to resist the CFRP plate from sliding, further increasing the pre-tensioning torque brings negative effect to the anchor because it causes severe pressure concentration and result in premature shear failure.
- (3) The presence of the cover plate completely alters the stress distribution to a more uniform mode and significantly improves the anchor efficiency. Therefore, the authors recommend Type B anchors proposed in this paper for both CFRP plate cables and structural strengthening.

CRedit authorship contribution statement

Jia-Qi Yang: Writing – review & editing, Writing – original draft, Methodology, Investigation, Funding acquisition, Conceptualization. **Husheng Wang:** Writing – original draft, Investigation. **Peng Feng:**

Writing – review & editing, Supervision, Funding acquisition. **Guozhen Ding:** Writing – review & editing, Methodology, Investigation. **Lili Wu:** Writing – review & editing, Supervision, Funding acquisition.

Declaration of Competing Interest

The authors declare that they have no known competing financial interests or personal relationships that could have appeared to influence the work reported in this paper.

Acknowledgements

This work is supported by the National Key Research and Development Program of China (2022YFC3801800), the Non-metallic Excellence and Innovation Centre for Building Materials (No. 2022TDA1-1), the National Natural Science Foundation of China (No. 52378207, 51908322, 52178177), and the Yueqi Distinguished Scholar Award Scheme of China University of Mining and Technology (Beijing) (No. 2602021RC59).

Data Availability

Data will be made available on request.

References

- [1] J.G. Teng, J.F. Chen, S.T. Smith, L. Lam, R.C. FRP-strengthened, structures, Wiley, London, UK, 2002.
- [2] Y. Liu, B. Zwingmann, M. Schlaich, Carbon fibre reinforced polymer for cable structures—a review, *Polymers* 7 (10) (2015) 2078–2099.
- [3] F.M. Mohee, A. Al-Mayah, A. Plumtree, Anchors for CFRP plates: State-of-the-art review and future potential, *Compos. Part B: Eng.* 90 (2016) 432–442.
- [4] Y. Yang, M.F. Fahmy, S. Guan, Z. Pan, Y. Zhan, T. Zhao, Properties and applications of FRP cable on long-span cable-supported bridges: A review, *Compos. Part B: Eng.* 190 (2020) 107934.
- [5] U. Meier, Proposal for a carbon fibre reinforced composite bridge across the Strait of Gibraltar at its narrowest site, *Proc. Inst. Mech. Eng., Part B: Manag. Eng. Manuf.* 201 (2) (1987) 73–78.
- [6] U. Meier, Carbon fibre reinforced polymer cables: Why? Why not? What if? *Arab. J. Sci. Eng.* 37 (2012) 399–411.
- [7] F. Matta, A. Nanni, A. Abdelrazaq, D. Gremel, R. Koch, Externally post-tensioned carbon FRP bar system for deflection control, *Constr. Build. Mater.* 23 (4) (2009) 1628–1639.
- [8] W.W. Wang, J.G. Dai, K.A. Harries, Q.H. Bao, Prestress losses and flexural behaviour of reinforced concrete beams strengthened with posttensioned CFRP sheets, *J. Compos. Constr.* 16 (2) (2012) 207–216.
- [9] H. Peng, J. Zhang, S. Shang, Y. Liu, C.S. Cai, Experimental study of flexural fatigue performance of reinforced concrete beams strengthened with prestressed CFRP plates, *Eng. Struct.* 127 (2016) 62–72.
- [10] J.Q. Yang, P. Feng, B. Liu, H. Wang, W. Zhao, L. Hu, Strengthening RC beams with mid-span supporting prestressed CFRP plates: An experimental investigation, *Eng. Struct.* 272 (2022) 115022.
- [11] Y. Liu, J.Z. Xie, T. Tafsirojjaman, Q.R. Yue, C. Tan, G.J. Che, CFRP lamella stay-cable and its force measurement based on microwave radar, *Case Stud. Constr. Mater.* 16 (2022) e00824.
- [12] P. Ai, P. Feng, H. Lin, P. Zhu, G. Ding, Novel self-anchored CFRP cable system: Concept and anchorage behaviour, *Compos. Struct.* 263 (2021) 113736.
- [13] J.W. Schmidt, A. Bennitz, B. Täljsten, P. Goltermann, H. Pedersen, Mechanical anchorage of FRP tendons—a literature review, *Constr. Build. Mater.* 32 (2012) 110–121.
- [14] P. Feng, P. Zhang, X. Meng, L. Ye, Mechanical analysis of stress distribution in a carbon fibre-reinforced polymer rod bonding anchor, *Polymers* 6 (4) (2014) 1129–1143.
- [15] P. Zhuge, Y. Yu, C.S. Cai, Z.H. Zhang, Y. Ding, Mechanical behaviour and optimal design method for innovative CFRP cable anchor, *J. Compos. Constr.* 23 (1) (2019) 04018067.
- [16] Li W. Study on carbon fibre reinforced polymer parallel-plate cables and corrugated-plate anchorages. Master thesis, Tsinghua University, 2016.
- [17] Y. Duo, X. Liu, Q. Yue, H. Chen, A novel variable curvature clamping anchor for the multilayer CFRP plate cable: Concept, numerical investigation, and design proposals, *Structures* 43 (2022) 164–177.
- [18] C. Liang, Z. Zhu, G. Bai, Y. Chen, W. Wang, T. Sun, Y. Xue, X. Liu, *Steel Struct. Des. Stad. Sanya Int. Sports Ind. Park. Build. Struct.* 51 (19) (2021) 18–24 (in Chinese).
- [19] C.G. Li, G.J. Xian, Novel wedge-shaped bond anchorage system for pultruded CFRP plates, *Mater. Struct.* 51 (2018) 1–4.
- [20] H. Ye, C. Liu, S. Hou, T. Wang, X. Li, Design and experimental analysis of a novel wedge anchor for prestressed CFRP plates using pre-tensioned bolts, *Compos. Struct.* 206 (2018) 313–325.

- [21] A. Hosseini, E. Ghafoori, M. Motavalli, A. Nussbaumer, X.L. Zhao, R. Al-Mahaidi, G. Terrasi, Development of prestressed unbonded and bonded CFRP strengthening solutions for tensile metallic members, *Eng. Struct.* 181 (2019) 550–561.
- [22] R. Suter, Jungo D. Prestressed CFRP strips for strengthening structures, *Beton-und Stahlbetonbau* 96 (5) (2001) 350–358 (in German).
- [23] Andra H.P., Maier M. 2000. Post-strengthening with externally bonded prestressed CFRP strips. IABSE Congress Report, 1507- 1514. Lucerne, Switzerland: International Association for Bridge and Structural Engineering.
- [24] B. Piatek, T. Siwowski, J. Michalowski, S. Blazewicz, Flexural strengthening of RC beams with prestressed CFRP strips: Development of novel anchor and tensioning system, *J. Compos. Constr.* 24 (3) (2020) 04020015.
- [25] H. Fan, A.P. Vassilopoulos, T. Keller, Pull-out behaviour of CFRP ground anchors with two-strap ends. *Compos. Struct.* 160 (2017 Jan 15) 1258–1267.
- [26] L. Hu, W. Li, P. Feng, Long-term behaviour of CFRP plates under sustained loads, *Adv. Struct. Eng.* 25 (5) (2022) 939–953.
- [27] J. Zhuo, T.N. Li, Mechanism of an innovative wave-shape-teeth-grip anchor of FRP sheets, *China Civ. Eng. J.* 38 (2005) 49–53.
- [28] G.G. Portnov, V.L. Kulakov, A.K. Arnautov, Grips for the transmission of tensile loads to a FRP strip, *Mech. Compos. Mater.* 49 (2013) 457–474.
- [29] G. Ding, P. Feng, Y. Wang, P. Ai, Novel pre-clamp lap joint for CFRP plates: Design and experimental study, *Compos. Struct.* 302 (2022) 116240.
- [30] GB/T 3354–2014. Test method for tensile properties of oriented fibre reinforced polymer matrix composites. 2014. (In Chinese).
- [31] G. Ding, P. Feng, Y. Wang, P. Ai, Q. Wang, Long-term bolt preload relaxation and contact pressure distribution in clamping anchorages for CFRP plates, *Compos. Struct.* 329 (2024) 117780.
- [32] Wu Y. Study on performance of prestressed CFRP plate anchorage system. Master Thesis. Chongqing University, 2016.
- [33] D.X. Cheng. Handbook of Mechanical Design, 6th Edition, Chemical Industry Press, Beijing, China, 2016.